Applied Mathematics and Computation 361 (2019) 517–535

Contents lists available at ScienceDirect

Applied Mathematics and Computation

journal homepage: www.elsevier.com/locate/amc

Mathematical analysis of a cholera infection model with vaccination strategy

Xiaohong Tian[a,b], Rui Xu[a,b,*], Jiazhe Lin[c]

[a] Complex Systems Research Center, Shanxi University, Taiyuan, Shanxi, 030006, PR China
[b] Shanxi Key Laboratory of Mathematical Techniques and Big Data Analysis on Disease Control and Prevention, Shanxi University, Taiyuan, Shanxi, 030006, PR China
[c] Institute of Applied Mathematics, Army Engineering University, Shijiazhuang, Hebei, 050003, PR China

ARTICLE INFO

MSC:
34K20
92D30

Keywords:
Cholera infection
Waning vaccine-induced immunity
Lyapunov function
Global stability
Optimal control

ABSTRACT

In this paper, a cholera infection model with vaccination strategy is investigated. By analyzing corresponding characteristic equations, the local stability of each of feasible equilibria is established. By means of Lyapunov functions and LaSalle's invariance principle, it is proved that if the basic reproduction number is less than unity, the disease-free equilibrium is globally asymptotically stable. If the basic reproduction number is greater than unity, the endemic equilibrium is globally asymptotically stable. In addition, by using Pontryagin's maximum principle, several reasonable optimal control strategies are suggested to the prevention and control of the cholera infection. Numerical simulations are carried out to illustrate the theoretical results.

1. Introduction

Cholera is a typical type of vector-borne disease. It is an acute, diarrheal illness caused by infection of the intestine with the bacterium Vibrio cholerae. Cholera outbreaks are generally associated to contaminated food and water supplies. An infected person experiences severe vomiting, explosive diarrhea and severe dehydration. Without immediate medical treatment, cholera may result in death within four to twelve hours after symptoms begin [1,2]. Beginning in April 2017, a major cholera epidemic occurred in Yemen. The World Health Organization (WHO) reports that there has claimed 1500 lives and sickened about 246,000 people since April, and the deterioration of health systems and its associated sanitation infrastructure are the main reasons of the cholera outbreak in Yemen [3].

V. cholera bacterium may be present in large numbers in various aquatic environments such as brackish (saltwater) rivers and coastal waters, and depend on the influence of external environments. In recent years, many works have been developed for cholera infection using ordinary differential equation models. In [4], by assuming that water-borne is the only route of transmission, Capasso and Paveri-Fontana proposed a basic cholera infection model describing the dynamics of infected people in the community and the dynamics of the aquatic population of pathogenic bacteria. In [5], Colwell and Huq pointed out that V. cholerae cells do not necessarily die when discharged into aquatic environments, but instead remain viable, and capable of transforming into a "culturable state". Based on the work of Capasso and Paveri-Fontana[4], in [6], Codeço proposed a cholera epidemic model that incorporates the environmental component, i.e. the V. cholerae

* Corresponding author at: Complex Systems Research Center, Shanxi University Taiyuan, Shanxi 030006, PR China.
E-mail address: xurui@sxu.edu.cn (R. Xu).

https://doi.org/10.1016/j.amc.2019.05.055
0096-3003/

concentration in the water supply, into a regular SIR epidemiological model:

$$\begin{aligned}
\dot{S}(t) &= \mu N - a\lambda(B)S(t) - \mu S(t),\\
\dot{I}(t) &= a\lambda(B)S(t) - \gamma I(t),\\
\dot{B}(t) &= \xi I(t) - \delta B(t),\\
\dot{R}(t) &= \gamma I(t) - \mu R(t),
\end{aligned} \tag{1.1}$$

where $S(t)$ represents the number of individuals who are susceptible to the disease, $I(t)$ the number of infected individuals, $R(t)$ the number of members who have been removed from the possibility of infection through full immunity, and $B(t)$ the concentration of toxigenic V. cholerae in water. N stands for the total human population, μ denotes the natural human birth/death rate. Infected people recover at rate γ. Cholera-infected individuals contribute to V. cholerae in the aquatic environment at rate ξ and vibrios have a net death rate δ in the environment. Susceptible individual becomes infected at a rate $a\lambda(B)$, where a is the rate of contact with untreated water and $\lambda(B)$ is the probability of such person to catch cholera. Further, as argued by Sengupta et al. only enough inoculum of V. cholerae can lead to cholera, probability of catching cholera ($\lambda(B)$) depends on the concentration of V. cholerae in the consumed water and this dependence is represented by a logistic dose response curve [7]. To place the model on more sound biological grounds, in [6], Codeço proposed the following nonlinear infectious incidence force function

$$\lambda(B) = \frac{B}{K+B},$$

here, K is the concentration of V. cholerae in contaminated water that yields 50% chance of catching cholera in the environment. In [6], it was found that environmental factors such as floods, droughts, seasonal variations of water temperature, and biological interactions may have potentially different effects on the spread of cholera. Recently, great attention has been paid to mathematical modelling of cholera infection with nonlinear incidence (see, for example, [8–14]).

However, we note that the effect of vaccination was ignored in above models. As far as we know, the main measures for the prevention and control of cholera in the long term is dependent on access to safe water, adequate sanitation, and basic hygiene needs. However, in most epidemic areas of cholera outbreaks, these problems are difficult to improve in the short term. In this case, vaccines provide an immediate alternative for the control of cholera. In 2010, WHO made formal recommendations on the use of oral cholera vaccine in complex emergencies and endemic settings [33]. Analysis of the experimental data in Bangladesh has shown that use of oral cholera vaccines conferred significant herd protection, through diminished risk of infection among nonvaccinees and enhanced protection of vaccinees who reside in vaccinated neighborhoods [15]. In recent years, there have been some works on cholera infection models with vaccination in the literature (see, for example, [16–20]). In [16], by using optimal control theory and Pontrjagin's maximum principle, Liao and Yang studied the optimal control strategy for cholera epidemic model with vaccination. Numerical simulation suggested that vaccination is the effective method of preventing and controlling the cholera infection. In [19], Posny et al. considered vaccination in the model of Mukandavire et al. [11]. It was pointed out that although vaccine may not be always completely effective, it can still be used as an effective method to control cholera infection.

Motivated by the works of Codeço [6] and Posny et al. [19], in this paper, we are concerned with the combined effects of environment-to-human transmission, nonlinear incidence and waning vaccine-induced immunity on the global dynamics of cholera infection. To this end, we consider the following differential equations:

$$\begin{aligned}
\dot{S}(t) &= A - \phi S(t) - \frac{\beta S(t)B(t)}{K+B(t)} - \mu S(t) + \eta V(t),\\
\dot{V}(t) &= \phi S(t) - \frac{\sigma\beta V(t)B(t)}{K+B(t)} - (\mu+\eta)V(t),\\
\dot{I}(t) &= \frac{\beta S(t)B(t)}{K+B(t)} + \frac{\sigma\beta V(t)B(t)}{K+B(t)} - (\mu+\gamma+d)I(t),\\
\dot{B}(t) &= \xi I(t) - \delta B(t),\\
\dot{R}(t) &= \gamma I(t) - \mu R(t),
\end{aligned} \tag{1.2}$$

where $S(t)$, $V(t)$, $I(t)$ and $R(t)$ denote the numbers of the susceptible, vaccinated, infectious and recovery individuals at time t, respectively. $B(t)$ denotes the concentration of toxigenic V. cholerae in water. The parameters β, γ, δ, μ, η, ϕ, σ, ξ, A and K are positive constants. A is the birth rate of newborns, μ is the natural human death rate, d is the per capita disease-induced death rate, β is the transmission coefficient of contact with untreated water. Here, the vaccine is assumed to be imperfect, vaccinated individuals also acquire infection via contact with symptomatic individuals. In this case, the effective contact rate, β, is multiplied by a scaling factor σ, where $0 \le \sigma \le 1$ is the efficacy of the vaccine so that $\sigma = 0$ means that the vaccine is completely effective in preventing infection, $0 < \sigma < 1$ means that the vaccine is not completely effective, and that the vaccinated individuals have only partial immunity, while $\sigma = 1$ means that the vaccine is utterly ineffective. The susceptible population is vaccinated at a constant rate ϕ, and the vaccine also wears off at a constant rate η. The corresponding flowchart of cholera transmission in system (1.2) is depicted in Fig. 1, variables and parameters in system (1.2) are listed in Tab. 1.

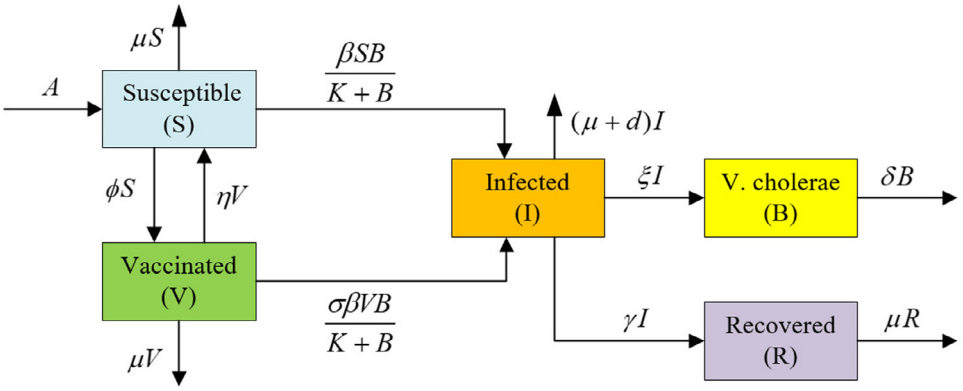

Fig. 1. Flowchart of cholera transmission in system (1.2).

The initial condition for system (1.2) takes the form

$$S(0) \geq 0, \quad V(0) \geq 0, \quad I(0) \geq 0, \quad B(0) \geq 0, \quad R(0) \geq 0. \tag{1.3}$$

It is easy to show that all solutions of system (1.2) with initial condition (1.3) are defined on $[0, +\infty)$ and remain positive for all $t \geq 0$.

The organization of this paper is as follows. In Section 2, by analyzing the corresponding characteristic equations, we study the local stability of each of the feasible equilibria of system (1.2). In Section 3, by means of suitable Lyapunov functions and LaSalle's invariance principle, we discuss the global stability of the disease-free equilibrium and the endemic equilibrium, respectively. In Section 4, we carry out a study of optimal control to seek cost-effective solutions of control strategies for cholera. In Section 5, we present numerical simulations to illustrate our results and study the effect of vaccination rate and the waning rate of vaccine on the dynamics of cholera infection, respectively. Besides, we shall perform a sensitivity analysis of basic reproduction number and get the optimal control solution by forward-backward sweep method. Finally, a brief discussion is given in Section 6 to end this work.

2. Equilibria and local stability

In this section, we study the existence of each of feasible equilibria of system(1.2), and establish their local stability by analyzing the corresponding characteristic equations, respectively.

Clearly, system (1.2) always has a disease-free equilibrium $E^0(S_0, V_0, 0, 0, 0)$, where

$$S_0 = \frac{A(\mu+\eta)}{\mu(\mu+\eta+\phi)}, \quad V_0 = \frac{A\phi}{\mu(\mu+\eta+\phi)}. \tag{2.1}$$

By means of the method of the next generation matrix (see, for example, van den Driessche and Watmough in [21]), the associated next generation matrices are given by

$$F = \begin{pmatrix} 0 & \frac{\beta S_0}{K} + \frac{\sigma\beta V_0}{K} \\ 0 & 0 \end{pmatrix}$$

and

$$V = \begin{pmatrix} \mu+\gamma+d & 0 \\ -\xi & \delta \end{pmatrix},$$

one obtains the basic reproduction number of system (1.2) as follows:

$$\mathscr{R}_0 = \rho(FV^{-1}) = \frac{A\beta\xi(\mu+\eta+\sigma\phi)}{K\delta\mu(\mu+\gamma+d)(\mu+\eta+\phi)],}$$

which represents the average number of secondary infections infected by an individual of infectives during whose whole course of disease in the case that all the members of the population are susceptible.

It is easy to show that if $\mathscr{R}_0 > 1$, in addition to the disease-free equilibrium E^0, system (1.2) has an endemic equilibrium $E^*(S^*, V^*, I^*, B^*, R^*)$, where

$$S^* = \frac{A[(\mu+\eta)(K+B^*)+\sigma\beta B^*](K+B^*)}{[(\mu+\eta)(K+B^*)+\sigma\beta B^*][(\mu+\phi)(K+B^*)+\beta B^*]-\phi\eta(K+B^*)^2},$$

$$V^* = \frac{A\phi}{[(\mu+\eta)(K+B^*)+\sigma\beta B^*][(\mu+\phi)(K+B^*)+\beta B^*]-\phi\eta(K+B^*)^2},$$

$$I^* = \frac{\delta}{\xi}B^*, \quad B^* = \frac{-A_2 + \sqrt{A_2^2 - 4A_1A_3}}{2A_1}, \quad R^* = \frac{\gamma}{\mu}I^*, \tag{2.2}$$

here

$$A_1 = \delta(\mu+\gamma+d)[\phi(\mu+\sigma\beta)+(\mu+\beta)(\mu+\eta+\sigma\beta)],$$
$$A_2 = K\delta(\mu+\gamma+d)[2\mu(\mu+\eta+\phi)+\sigma\beta(\mu+\phi)+\beta(\mu+\eta)] - A\beta\xi[\mu+\eta+\sigma(\beta+\phi)],$$
$$A_3 = K^2\mu\delta(\mu+\gamma+d)(\mu+\eta+\phi)(1-\mathscr{R}_0).$$

We now give a result on the local stability of the disease-free equilibrium E^0 and the endemic equilibrium E^* of system (1.2).

Theorem 2.1. *For system (1.2), we have*

(i) *If $\mathscr{R}_0 < 1$, the disease-free equilibrium $E^0(S_0, V_0, 0, 0, 0)$ is locally asymptotically stable and is unstable if $\mathscr{R}_0 > 1$.*
(ii) *If $\mathscr{R}_0 > 1$, the endemic equilibrium $E^*(S^*, V^*, I^*, B^*, R^*)$ exists and is locally asymptotically stable.*

Proof. The characteristic equation of system (1.2) at the disease-free equilibrium E^0 is of the form

$$(\lambda+\mu)f_1(\lambda)f_2(\lambda) = 0, \tag{2.3}$$

where

$$f_1(\lambda) = \lambda^2 + (2\mu+\eta+\phi)\lambda + \mu(\mu+\eta+\phi),$$
$$f_2(\lambda) = \lambda^2 + (\mu+\gamma+d+\delta)\lambda + \delta(\mu+\gamma+d)(1-\mathscr{R}_0).$$

Clearly, Eq. (2.3) always has three negative real roots. Other roots of Eq. (2.3) are determined by the equation $f_2(\lambda) = 0$. If $\mathscr{R}_0 < 1$, it is easy to show that roots of $f_2(\lambda) = 0$ have only negative real parts. Accordingly, the equilibrium E^0 of system (1.2) is locally asymptotically stable. If $\mathscr{R}_0 > 1$, Eq. (2.3) has at least one positive real root. Therefore, E^0 is unstable.

The characteristic equation of system (1.2) at the endemic equilibrium E^* takes the form

$$(\lambda+\mu)\left(\lambda^4 + P_3\lambda^3 + P_2\lambda^2 + P_1\lambda + P_0\right) = 0, \tag{2.4}$$

where

$$P_0 = \delta(\mu+\gamma+d)\left(\mu+\phi+\frac{\beta B^*}{K+B^*}\right)\left(\mu+\frac{\sigma\beta B^*}{K+B^*}\right) + \eta\delta(\mu+\gamma+d)(\mu+\beta)\frac{B^*}{K+B^*}$$
$$- \xi\mu\frac{K\beta S^*}{(K+B^*)^2}\left(\mu+\phi+\frac{\sigma\beta B^*}{K+B^*}\right) - \xi\mu\frac{K\sigma\beta V^*}{(K+B^*)^2}\left(\mu+\phi+\frac{\beta B^*}{K+B^*}\right),$$
$$P_1 = \delta(\mu+\gamma+d)\frac{B^*}{K+B^*}\left(2\mu+\phi+\eta+\frac{\beta B^*}{K+B^*}+\frac{\sigma\beta B^*}{K+B^*}\right) + \xi\frac{K\beta^2B^*}{(K+B^*)^3}(S^*+\sigma^2V^*)$$
$$+ (\mu+\gamma+d+\delta)\left[\left(\mu+\phi+\frac{\beta B^*}{K+B^*}\right)\left(\mu+\frac{\sigma\beta B^*}{K+B^*}\right) + \left(\mu+\frac{\beta B^*}{K+B^*}\right)\eta\right],$$
$$P_2 = \left(\mu+\phi+\frac{\beta B^*}{K+B^*}\right)\left(\mu+\frac{\sigma\beta B^*}{K+B^*}\right) + \left(\mu+\frac{\beta B^*}{K+B^*}\right)\eta + \delta(\mu+\gamma+d)\frac{B^*}{K+B^*}$$
$$+ (\mu+\gamma+d+\delta)\left(2\mu+\phi+\eta+\frac{\beta B^*}{K+B^*}+\frac{\sigma\beta B^*}{K+B^*}\right),$$
$$P_3 = 3\mu+\gamma+d+\delta+\phi+\eta+\frac{\beta B^*}{K+B^*}+\frac{\sigma\beta B^*}{K+B^*}.$$

Denote

$$\Delta_1 = P_3, \quad \Delta_2 = P_2P_3 - P_1, \quad \Delta_3 = P_1P_2P_3 - P_0P_3^2 - P_1^2.$$

Clearly, $\Delta_1 > 0$. A direct calculation shows that

$$\Delta_2 = \delta B_6\left[2\mu+\phi+\eta+\frac{B^*}{K+B^*}(\delta+B_4+B_6)\right] + \xi\frac{K\sigma\beta^2B^*}{(K+B^*)^3}(S^*+V^*)$$
$$+ B_5\left[\delta^2 + B_1B_2 + (\delta+B_6)(B_5+B_6) + B_3\eta\right] > 0,$$

and

$$\Delta_3 = \delta\mu\eta B_6[(2\mu+\phi+\eta)(2\delta+B_6)+\delta B_4] + \delta\mu\eta B_5(B_5+B_6) + \delta^2B_5^2\left[B_1B_2 + B_3\eta + \delta B_6\frac{B^*}{K+B^*}\right]$$

$$
\begin{aligned}
&+\delta B_6(\delta+B_6)(\mu\eta+B_1B_2)(B_4+B_6)\frac{B^*}{K+B^*}\\
&+\delta B_6B_5^2\frac{B^*}{K+B^*}\left[B_1B_2+\frac{\eta\beta B^*}{K+B^*}+2(\delta+B_6)(B_5+B_6)\right]\\
&+(\delta+B_6)(B_1B_2+B_3\eta)^2B_5\left[\delta^2+2B_6(B_5+B_6)\right]\\
&+\delta^2B_6^2\frac{B^*}{K+B^*}B_5\left[2\mu+\phi+\eta+\frac{B^*}{K+B^*}(\delta+B_4+B_6)\right]\\
&+\frac{\xi K\beta^2B^*}{(K+B^*)^3}\left[S^*\delta^2B_1+\sigma^2V^*\delta^2(\eta+B_2)+\sigma V^*\mu\eta(\delta+B_6)\right]\\
&+\frac{2\xi K\beta^2B^*}{(K+B^*)^3}(S^*+\sigma^2V^*)B_5[B_1B_2+B_3\eta]\\
&+\frac{\xi K\beta S^*}{(K+B^*)^2}\mu(\mu+\phi)(\delta+B_6)(2\mu+\phi+\eta+B_5)\\
&+\frac{\xi K\beta^2S^*B^*}{(K+B^*)^3}\delta B_6\left[\mu+\phi+\frac{\beta B^{*2}}{(K+B^*)^2}+\frac{\sigma B^*}{K+B^*}B_5\right]\\
&+\frac{\xi K\sigma^2\beta^2V^*B^*}{(K+B^*)^3}\delta B_6\left[2\mu+\phi+\eta+\frac{B^*}{K+B^*}(\delta+B_4+B_6)\right]\\
&+\frac{\xi K\sigma\beta^2S^*B^*}{(K+B^*)^3}(\delta+B_6)[\mu(\mu+\phi+B_5)+B_3\eta]\\
&+\frac{\xi K\beta\mu B_1}{(K+B^*)^2}(S^*+\sigma V^*)\left[(\delta+B_5+B_6)B_5+B_5^2+(2\mu+\phi+\eta)(\delta+B_6)\right]\\
&+\frac{\xi K\beta^2S^*B^*}{(K+B^*)^3}(\delta+B_6)B_1(B_5+B_6)\\
&+\frac{\xi K\beta^2S^*B^*}{(K+B^*)^3}(\delta+B_6)\left[\mu(4\mu+2\phi+\eta+B_1+B_5)+\frac{\sigma\beta B^*}{K+B^*}(\mu+\eta+B_2)\right]\\
&+\frac{\xi K\sigma^2\beta^2V^*B^*}{(K+B^*)^3}(\delta+B_6)[(\eta+B_2)(B_5+B_6)+B_1(\mu+B_1)]>0,
\end{aligned}
$$

here

$$
\begin{aligned}
&B_1=\mu+\phi+\frac{\beta B^*}{K+B^*},\quad B_2=\mu+\frac{\sigma\beta B^*}{K+B^*},\quad B_3=\mu+\frac{\beta B^*}{K+B^*}\\
&B_4=\frac{\beta B^*+\sigma\beta B^*}{K+B^*},\quad B_5=2\mu+\phi+\eta+B_4,\quad B_6=\mu+\gamma+d.
\end{aligned}
$$

Hence, by Routh-Hurwitz criterion, we see that the equilibrium E^* is locally asymptotically stable if $\mathscr{R}_0>1$. □

3. Global stability

In this section, we are concerned with the global stability of the endemic equilibrium $E^*(S^*, V^*, I^*, B^*, R^*)$ and the disease-free equilibrium $E^0(S_0, V_0, 0, 0, 0)$ of system (1.2). The technique of proofs is to use suitable Lyapunov functions and LaSalle's invariance principle.

Theorem 3.1. *If $\mathscr{R}_0>1$, then the endemic equilibrium $E^*(S^*, V^*, I^*, B^*, R^*)$ of system (1.2) is globally asymptotically stable.*

Proof. Let $(S(t), V(t), I(t), B(t), R(t))$ be any positive solution of system (1.2) with initial condition (1.3).

Define

$$
\begin{aligned}
L_1(t)&=S(t)-S^*-S^*\ln\frac{S(t)}{S^*}+V(t)-V^*-V^*\ln\frac{V(t)}{V^*}\\
&\quad+I(t)-I^*-I^*\ln\frac{I(t)}{I^*}+\frac{\mu+\gamma+d}{\xi}\left(B(t)-B^*-B^*\ln\frac{B(t)}{B^*}\right).
\end{aligned}\tag{3.1}
$$

Calculating the derivative of $L_1(t)$ along positive solutions of system (1.2), it follows that

$$\begin{aligned}\frac{\mathrm{d}}{\mathrm{d}t}L_1(t) &= \left(1-\frac{S^*}{S(t)}\right)\left[A-\phi S(t)-\frac{\beta S(t)B(t)}{K+B(t)}-\mu S(t)+\eta V(t)\right]\\ &+\left(1-\frac{V^*}{V(t)}\right)\left[\phi S(t)-\frac{\sigma\beta V(t)B(t)}{K+B(t)}-(\mu+\eta)V(t)\right]\\ &+\left(1-\frac{I^*}{I(t)}\right)\left[\frac{\beta S(t)B(t)}{K+B(t)}+\frac{\sigma\beta V(t)B(t)}{K+B(t)}-(u+\gamma+d)I(t)\right]\\ &+\frac{\mu+\gamma+d}{\xi}\left(1-\frac{B^*}{B(t)}\right)[\xi I(t)-\delta B(t)].\end{aligned} \tag{3.2}$$

On substituting $A=\frac{\beta S^*B^*}{K+B^*}+\frac{\sigma\beta V^*B^*}{K+B^*}+\mu S^*+\mu V^*$ into (3.2), we have

$$\begin{aligned}\frac{\mathrm{d}}{\mathrm{d}t}L_1(t) &= \frac{\beta S^*B^*}{K+B^*}+\frac{\sigma\beta V^*B^*}{K+B^*}+2\mu S^*+2\mu V^*+\eta V^*+\phi S^*+(\mu+\gamma+d)I^*\\ &+\frac{\delta(\mu+\gamma+d)}{\xi}B^*-\mu S^*\frac{S(t)}{S^*}-\mu S^*\frac{S^*}{S(t)}-\frac{\beta S^*B^*}{K+B^*}\frac{S^*}{S(t)}-\mu V^*\frac{S^*}{S(t)}\\ &-\frac{\sigma\beta V^*B^*}{K+B^*}\frac{S^*}{S(t)}-\eta V^*\frac{S^*}{S(t)}\frac{V(t)}{V^*}-\mu V^*\frac{V(t)}{V^*}-\phi S^*\frac{S(t)}{S^*}\frac{V^*}{V(t)}\\ &+\frac{\beta S(t)B(t)}{K+B(t)}\frac{S^*}{S(t)}+\frac{\sigma\beta V(t)B(t)}{K+B(t)}\frac{V^*}{V(t)}-\frac{\beta S(t)B(t)}{K+B(t)}\frac{I^*}{I(t)}\\ &-\frac{\sigma\beta V(t)B(t)}{K+B(t)}\frac{I^*}{I(t)}-\frac{\delta(\mu+\gamma+d)}{\xi}B^*\frac{B(t)}{B^*}-(\mu+\gamma+d)I^*\frac{I(t)}{I^*}\frac{B^*}{B(t)}.\end{aligned} \tag{3.3}$$

Noting that

$$\frac{\beta(S^*+\sigma V^*)B^*}{K+B^*}=(\mu+\gamma+d)I^*=\frac{\delta(\mu+\gamma+d)}{\xi}B^*,\quad \phi S^*=\frac{\sigma\beta V^*B^*}{K+B^*}+(\mu+\eta)V^*,$$

it follows from (3.3) that

$$\begin{aligned}\frac{\mathrm{d}}{\mathrm{d}t}L_1(t) &= \mu S^*\left(2-\frac{S^*}{S(t)}-\frac{S(t)}{S^*}\right)+\eta V^*\left(2-\frac{S^*}{S(t)}\frac{V(t)}{V^*}-\frac{S(t)}{S^*}\frac{V^*}{V(t)}\right)\\ &+\mu V^*\left(3-\frac{S^*}{S(t)}-\frac{V(t)}{V^*}-\frac{S(t)}{S^*}\frac{V^*}{V(t)}\right)\\ &+\frac{\beta S^*B^*}{K+B^*}\left(4-\frac{S^*}{S(t)}-\frac{I(t)}{I^*}\frac{B^*}{B(t)}-\frac{K+B(t)}{K+B^*}-\frac{S(t)}{S^*}\frac{B(t)}{B^*}\frac{I^*}{I(t)}\frac{K+B^*}{K+B(t)}\right)\\ &+\frac{\sigma\beta V^*B^*}{K+B^*}\left(5-\frac{S^*}{S(t)}-\frac{S(t)}{S^*}\frac{V^*}{V(t)}-\frac{I(t)}{I^*}\frac{B^*}{B(t)}-\frac{K+B(t)}{K+B^*}-\frac{V(t)}{V^*}\frac{B(t)}{B^*}\frac{I^*}{I(t)}\frac{K+B^*}{K+B(t)}\right)\\ &-\frac{K\beta(S^*+\sigma V^*)}{(K+B^*)^2(K+B(t))}(B(t)-B^*)^2.\end{aligned} \tag{3.4}$$

Since the arithmetic mean is greater than or equal to the geometric mean, it therefore follows from (3.4) that if $\mathscr{R}_0>1$, $L_1'(t)\le 0$ and the equalities hold only for $S=S^*, V=V^*, I=I^*$ and $B=B^*$. Let $\mathcal{M}$ be the largest invariant subset of the set $\Sigma=\{(S(t),V(t),B(t),I(t))|\ L_1'(t)=0\}$. Clearly, it follows from (3.4) that $L_1'(t)=0$ if and only if $(S(t),V(t),B(t),I(t))=(S^*,V^*,I^*,B^*)$. We obtain from the fifth equation of system (1.2) that $0=\dot{R}(t)=\gamma I^*-\mu R(t)$, which leads to $R=R^*$. Hence, the only invariant set in Σ is $\mathcal{M}=\{E^*\}$. From Section 2, we see that if $\mathscr{R}_0>1$, E^* is locally asymptotically stable. Accordingly, the global asymptotic stability of E^* of system (1.2) follows from LaSalle's invariance principle. This completes the proof. □

We now investigate the global stability of the disease-free equilibrium $E^0(S_0, V_0, 0, 0, 0)$ of system (1.2).

Theorem 3.2. *If $\mathscr{R}_0<1$, then the disease-free equilibrium $E^0(S_0, V_0, 0, 0, 0)$ of system (1.2) is globally asymptotically stable.*

Proof. Let $(S(t), V(t), I(t), B(t), R(t))$ be any positive solution of system (1.2) with initial condition (1.3).
Define

$$L_2(t)=S(t)-S_0-S_0\ln\frac{S(t)}{S_0}+V(t)-V_0-V_0\ln\frac{V(t)}{V_0}+I(t)+\frac{\mu+\gamma+d}{\xi}B(t). \tag{3.5}$$

Calculating the derivative of $L_2(t)$ along positive solutions of system (1.2), it follows that

$$\begin{aligned}\frac{\mathrm{d}}{\mathrm{d}t}L_2(t) &= \left(1-\frac{S_0}{S(t)}\right)\left[A-\phi S(t)-\frac{\beta S(t)B(t)}{K+B(t)}-\mu S(t)+\eta V(t)\right]\\ &\quad+\left(1-\frac{V_0}{V(t)}\right)\left[\phi S(t)-\frac{\sigma\beta V(t)B(t)}{K+B(t)}-(\mu+\eta)V(t)\right]\\ &\quad+\frac{\beta S(t)B(t)}{K+B(t)}+\frac{\sigma\beta V(t)B(t)}{K+B(t)}-(u+\gamma+d)I(t)+\frac{\mu+\gamma+d}{\xi}[\xi I(t)-\delta B(t)].\end{aligned} \tag{3.6}$$

On substituting $A=\mu S_0+\mu V_0, \phi S_0=(\mu+\eta)V_0$ into (3.6), we obtain that

$$\begin{aligned}\frac{\mathrm{d}}{\mathrm{d}t}L_2(t) &= \left(1-\frac{S_0}{S(t)}\right)\left[\mu S_0+\mu V_0-\phi S(t)-\frac{\beta S(t)B(t)}{K+B(t)}-\mu S(t)+\eta V(t)\right]\\ &\quad+\left(1-\frac{V_0}{V(t)}\right)\left[\phi S(t)-\frac{\sigma\beta V(t)B(t)}{K+B(t)}-(\mu+\eta)V(t)\right]\\ &\quad+\frac{\beta S(t)B(t)}{K+B(t)}+\frac{\sigma\beta V(t)B(t)}{K+B(t)}-\frac{\mu+\gamma+d}{\xi}\delta B(t)\\ &= 2\mu S_0+3\mu V_0+2\eta V_0-\mu S_0\frac{S(t)}{S_0}-\mu S_0\frac{S_0}{S(t)}-\mu V_0\frac{S_0}{S(t)}\\ &\quad-\eta V_0\frac{V(t)}{V_0}\frac{S_0}{S(t)}-\mu V_0\frac{V(t)}{V_0}-(\mu+\eta)V_0\frac{S(t)}{S_0}\frac{V_0}{V(t)}\\ &\quad+\frac{\beta S_0B(t)}{K+B(t)}+\frac{\sigma\beta V_0B(t)}{K+B(t)}-\frac{\mu+\gamma+d}{\xi}\delta B(t).\end{aligned} \tag{3.7}$$

It therefore follows from (3.7) that

$$\begin{aligned}\frac{\mathrm{d}}{\mathrm{d}t}L_2(t) &= \frac{K\delta(\mu+\gamma+d)B(t)}{\xi(K+B(t))}(\mathscr{R}_0-1)-\frac{\delta(\mu+\gamma+d)}{\xi(K+B(t))}B^2(t)+\mu S_0\left(2-\frac{S(t)}{S_0}-\frac{S_0}{S(t)}\right)\\ &\quad+\eta V_0\left(2-\frac{V(t)}{V_0}\frac{S_0}{S(t)}-\frac{S(t)}{S_0}\frac{V_0}{V(t)}\right)+\mu V_0\left(3-\frac{S_0}{S(t)}-\frac{V(t)}{V_0}-\frac{S(t)}{S_0}\frac{V_0}{V(t)}\right).\end{aligned} \tag{3.8}$$

Hence, if $\mathscr{R}_0<1$, we obtain from (3.8) that $L_2'(t)\le 0$. Therefore, solutions limit to $\mathcal{M}$, the largest invariant subset of $L_2'(t)=0$. Clearly, it follows from (3.8) that $L_2'(t)=0$ if and only if $S=S_0, V=V_0$ and $B=0$. Noting that $\mathcal{M}$ is invariant, for each element in $\mathcal{M}$, we have $B=0, B'(t)=0$. It therefore follows from the third equation of system (1.2) that

$$0=B'(t)=\xi I(t),$$

which yields $I=0$. Hence, $L_2'(t)=0$ if and only if $(S,V,I,B)=(S_0,V_0,0,0)$. Further, using a similar argument as that in the proof of Theorem 3.1, the global asymptotic stability of the disease-free equilibrium E^0 of system (1.2) follows from LaSalle's invariance principle. This completes the proof. □

4. Optimal control strategies

In this section, we apply Pontryagin's maximum principle to seek the suitable strategies for the optimal control of the cholera infection. The goal is to minimize the number of infected individuals and corresponding cost of the strategies during the epidemic. Control strategies, such as quarantine, vaccination, sanitation, can realize the control of cholera at different cost.

Define a control function set as $U=\{u_i|i=1,2,3,4\}$, where the meanings of u_i are listed as follows:

(1) u_1 is a kind of vaccination strategy that can increase the inoculation proportion of susceptible individuals;
(2) u_2 is a quarantine strategy which is used to reduce the contact among infected individuals;
(3) u_3 is another kind of vaccination strategy aimed at increasing the validity of inoculation;
(4) u_4 is a sanitation strategy aimed at killing vibrios in contaminated water.

We incorporate time dependent controls into the model (1.2) to determine the optimal strategy for controlling the disease, and consider the following nonlinear system:

$$\begin{aligned}\dot{S}(t) &= A-u_1(t)S(t)-\frac{\beta(1-u_2(t))S(t)B(t)}{K+B(t)}-\mu S(t)+\eta(1-u_3(t))V(t),\\ \dot{V}(t) &= u_1(t)S(t)-\frac{\sigma\beta(1-u_2(t))V(t)B(t)}{K+B(t)}-[\mu+\eta(1-u_3(t))]V(t),\\ \dot{I}(t) &= (S(t)+\sigma V(t))\frac{\beta(1-u_2(t))B(t)}{K+B(t)}-(\mu+\gamma+d)I(t),\end{aligned}$$

$$\dot{B}(t) = \xi I(t) - (\delta + u_4(t))B(t),$$
$$\dot{R}(t) = \gamma I(t) - \mu R(t). \tag{4.1}$$

The objective functional is

$$J(X(\cdot), U(\cdot)) = \int_0^T \left(AI + \frac{B_1}{2}{u_1}^2 + \frac{B_2}{2}{u_2}^2 + \frac{B_3}{2}{u_3}^2 + \frac{B_4}{2}{u_4}^2\right)\mathrm{d}t,$$

where A denotes the weight constant of the infected individuals, B_1, B_2, B_3 and B_4 are the weight constants for the control strategies. $B_1{u_1}^2/2$, $B_2{u_2}^2/2$, $B_3{u_3}^2/2$ and $B_4{u_4}^2/2$ describe the cost associated with increasing inoculation proportion, quarantine, increasing inoculation validity, and sanitation strategies, respectively. The square of the control variables shows the severity of the side effects of the four strategies [22]. Due to the limitation of medical technology or cost, we assume that the control function $u_i (i = 1, 2, 3, 4)$ are bounded, and belong to a set of admissible controls

$$\mathcal{U} = \left\{U(\cdot) \in L^\infty\left([0, T]; \mathbb{R}^4\right) | 0 < u_i \le u_{i\max} < 1, \forall t \in [0, T]\right\}.$$

Denote $X = (S, V, I, B, R)$, and the set $\mathcal{X}$ of admissible trajectories is given by

$$\mathcal{X} = \left\{X(\cdot) \in W^{1,1}\left([0, T]; \mathbb{R}^5\right) | X(\cdot) \text{ satisfies (1.3) and (4.1)}\right\}.$$

We now find an optimal control $U^\star(\cdot) \in \mathcal{U}$ and a corresponding optimal state $X^\star(\cdot) = (S^\star(\cdot), V^\star(\cdot), I^\star(\cdot), B^\star(\cdot), R^\star(\cdot)) \in \mathcal{X}$ on time interval [0, T], and minimizing the objective functional J, i.e.,

$$J(X^\star(\cdot), U^\star(\cdot)) = \min_{X(\cdot), U(\cdot) \in \mathcal{X} \times \mathcal{U}} J(X(\cdot), U(\cdot)). \tag{4.2}$$

According to Pontryagin's maximum principle [23], if $U(\cdot) \in \mathcal{U}$ is optimal for problem (4.2) with fixed final time T, then there exists a nontrivial absolutely continuous mapping $\lambda : [0, T] \to \mathbb{R}^5$, $\lambda(t) = (\lambda_1(t), \lambda_2(t), \lambda_3(t), \lambda_4(t), \lambda_5(t))$, called the adjoint vector, such that

(1) the control system:

$$S' = \frac{\partial H}{\partial \lambda_1}, \quad V' = \frac{\partial H}{\partial \lambda_2}, \quad I' = \frac{\partial H}{\partial \lambda_3}, \quad B' = \frac{\partial H}{\partial \lambda_4}, \quad R' = \frac{\partial H}{\partial \lambda_5};$$

(2) the adjoint system:

$${\lambda_1}' = -\frac{\partial H}{\partial S}, \quad {\lambda_2}' = -\frac{\partial H}{\partial V}, \quad {\lambda_3}' = -\frac{\partial H}{\partial I}, \quad {\lambda_4}' = -\frac{\partial H}{\partial B}, \quad {\lambda_5}' = -\frac{\partial H}{\partial R};$$

(3) the minimization condition:

$$H(X^\star(t), U^\star(t), \lambda^\star(t)) = \min_{0 < u_i \le u_{i\max}} H(X^\star(t), U(t), \lambda^\star(t))$$

hold for almost all $t \in [0, T]$, where the function H is defined by

$$\begin{aligned} H(X, U, \lambda) = {} & AI + \frac{B_1}{2}{u_1}^2 + \frac{B_2}{2}{u_2}^2 + \frac{B_3}{2}{u_3}^2 + \frac{B_4}{2}{u_4}^2 \\ & + \lambda_1\left[A - u_1 S - \frac{\beta(1-u_2)SB}{K+B} - \mu S + \eta(1-u_3)V\right] \\ & + \lambda_2\left\{u_1 S - \frac{\sigma\beta(1-u_2)VB}{K+B} - [\mu + \eta(1-u_3)]V\right\} \\ & + \lambda_3\left[(S + \sigma V)\frac{\beta(1-u_2)B}{K+B} - (\mu + \gamma + d)I\right] \\ & + \lambda_4[\xi I - (\delta + u_4)B] + \lambda_5(\gamma I - \mu R), \end{aligned}$$

which is called the Hamiltonian.

Further, the following transversality conditions also hold:

$$\lambda_i(T) = 0, \quad i = 1, \ldots, 5.$$

From [23–27], it is not difficult to show the following result.

Theorem 4.1. *The optimal control problem (4.2) with fixed final time T admits a unique optimal solution $(S^\star(\cdot), V^\star(\cdot), I^\star(\cdot), B^\star(\cdot), R^\star(\cdot))$ associated with an optimal control $U(t)$ for $t \in [0, T]$. Moreover, there exist adjoint functions ${\lambda_i}^\star(\cdot)(i = 1, \ldots, 5)$, such that*

$$\frac{\mathrm{d}\lambda_1^\star}{\mathrm{d}t} = (\mu + u_1)\lambda_1^\star + \frac{\beta(1-u_2)B}{K+B}\lambda_1^\star - u_1\lambda_2^\star - \frac{\beta(1-u_2)B}{K+B}\lambda_3^\star,$$
$$\frac{\mathrm{d}\lambda_2^\star}{\mathrm{d}t} = -\eta(1-u_3)\lambda_1^\star + \frac{\sigma\beta(1-u_2)B}{K+B}\lambda_2^\star + [\mu + \eta(1-u_3)]\lambda_2^\star - \frac{\sigma\beta(1-u_2)B}{K+B}\lambda_3^\star,$$

Table 1
The definitions of the parameters in system (1.2).

Parameter	Description
A	Birth rate of newborns
ϕ	Vaccination rate
β	Environment-to-human transmission rate
K	Concentration of Vibrio Cholerae in environment
η	Waning rate of vaccine
μ	Natural human death rate
σ	The reduction of vaccine efficacy
γ	Recovery rate
d	Cholera-related death rate
ξ	Rate of human contribution to Vibrio Cholerae
δ	Death rate of the vibrios

$$\begin{aligned}
\frac{d\lambda_3^\star}{dt} &= (\mu+\gamma+d)\lambda_3^\star - \xi\lambda_4^\star - \gamma\lambda_5^\star - A,\\
\frac{d\lambda_4^\star}{dt} &= \frac{\beta(1-u_2)SK}{(K+B)^2}\lambda_1^\star + \frac{\sigma\beta(1-u_2)VK}{(K+B)^2}\lambda_2^\star - \frac{\beta(1-u_2)(S+\sigma V)K}{(K+B)^2}\lambda_3^\star + (\delta+u_4)\lambda_4^\star,\\
\frac{d\lambda_5^\star}{dt} &= \mu\lambda_5^\star,
\end{aligned} \tag{4.3}$$

with transversality conditions

$$\lambda_i{}^\star(T) = 0, \quad i = 1,\dots,5.$$

Furthermore,

$$u_i^\star = \max[0, \min(\tilde{u}_i, u_{i\max})], \tag{4.4}$$

where

$$\tilde{u}_1 = \frac{(\lambda_1^\star - \lambda_2^\star)S^\star}{B_1}, \quad \tilde{u}_2 = \frac{\beta S^\star B^\star(\lambda_3^\star - \lambda_1^\star) + \sigma\beta V^\star B^\star(\lambda_3^\star - \lambda_2^\star)}{B_2(K+B^\star)},$$
$$\tilde{u}_3 = \frac{\eta V^\star(\lambda_1^\star - \lambda_2^\star)}{B_3}, \quad \tilde{u}_4 = \frac{B^\star\lambda_4^\star}{B_4}.$$

In the next section, we discuss the numerical solutions of the optimality system. Numerical techniques for optimal control problems can often be classified as either direct or indirect. In terms of disease control, indirect methods, such as forward-backward sweep method, approximate solutions to optimal control problems by numerically solving the boundary value problem for the differential-algebraic system generated by the maximum principle [28]. The idea exploited by forward-backward sweep method is that the initial value problem of the state equation is solved forward in time, using an estimate for the control and costate variables, then the costate final value problem is solved backwards in time (see, for examples, [18,22,29]).

5. Numerical simulation

In this section, we give some numerical examples to illustrate the main results in Sections 2 and 4. Besides, we investigate the effect of vaccination rate and the waning rate of vaccine on the dynamics of cholera infection. Furthermore, sensitivity analysis is used to quantify the range of variability in basic reproduction number and to identify the key factors giving rise to reproduction number, which can be helpful to design treatment strategies. Finally, by forward-backward sweep method, we obtain the time-dependent optimal control strategies.

First, we choose appropriate parameters and simulate each of feasible equilibria, respectively.

Case 1: Corresponding parameters are listed in Case 1 of Table 1. It is easy to show that the reproduction number $\mathscr{R}_0 = 0.5002 < 1$. System (1.2) has a disease-free equilibrium E^0(612.7, 1212, 0, 0, 0). By Theorem 2.1, we see that E^0 is locally asymptotically stable. Numerical simulations illustrate this observation (see, Fig. 2).

Case 2: Corresponding parameters are listed in Case 2 of Table 1. Direct calculation shows that $\mathscr{R}_0 = 3.3274 > 1$. Hence, system (1.2) has a unique endemic equilibrium E^* (185.3,361.5,3.7,1114,268.4). By Theorem 2.1, we derive that the endemic equilibrium E^* is locally asymptotically stable (see, Fig. 3).

5.1. Effect of vaccination rate

In order to investigate the effect of vaccination rate, we carry out some numerical simulations to show the contribution of vaccination rate during the whole infection. From Fig. 4, we see that as vaccination rate ϕ increases, susceptible individuals

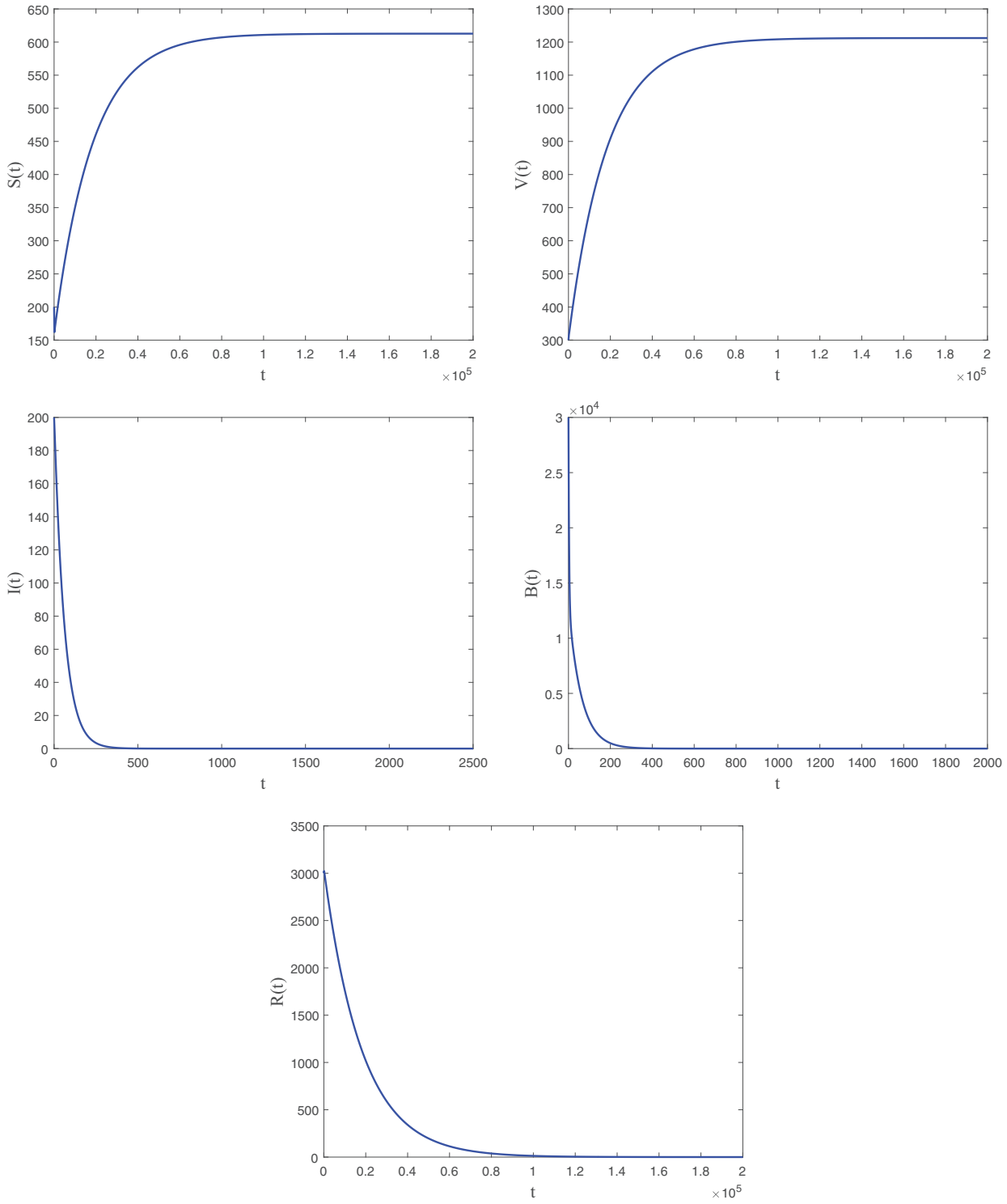

Fig. 2. The graph trajectories of $S(t)$, $V(t)$, $I(t)$, $B(t)$ and $R(t)$ versus t of system (1.2) where $\mathscr{R}_0 = 0.5002 < 1$. E^0 is locally asymptotically stable.

decreases while vaccinated individuals increases. The graph trajectories of infected individuals and pathogen population converge more slowly as ϕ increases, which implies that the increase of the vaccination rate can delay infection. Thus, to increase the vaccination rate is an effective means to control the infection progress of cholera.

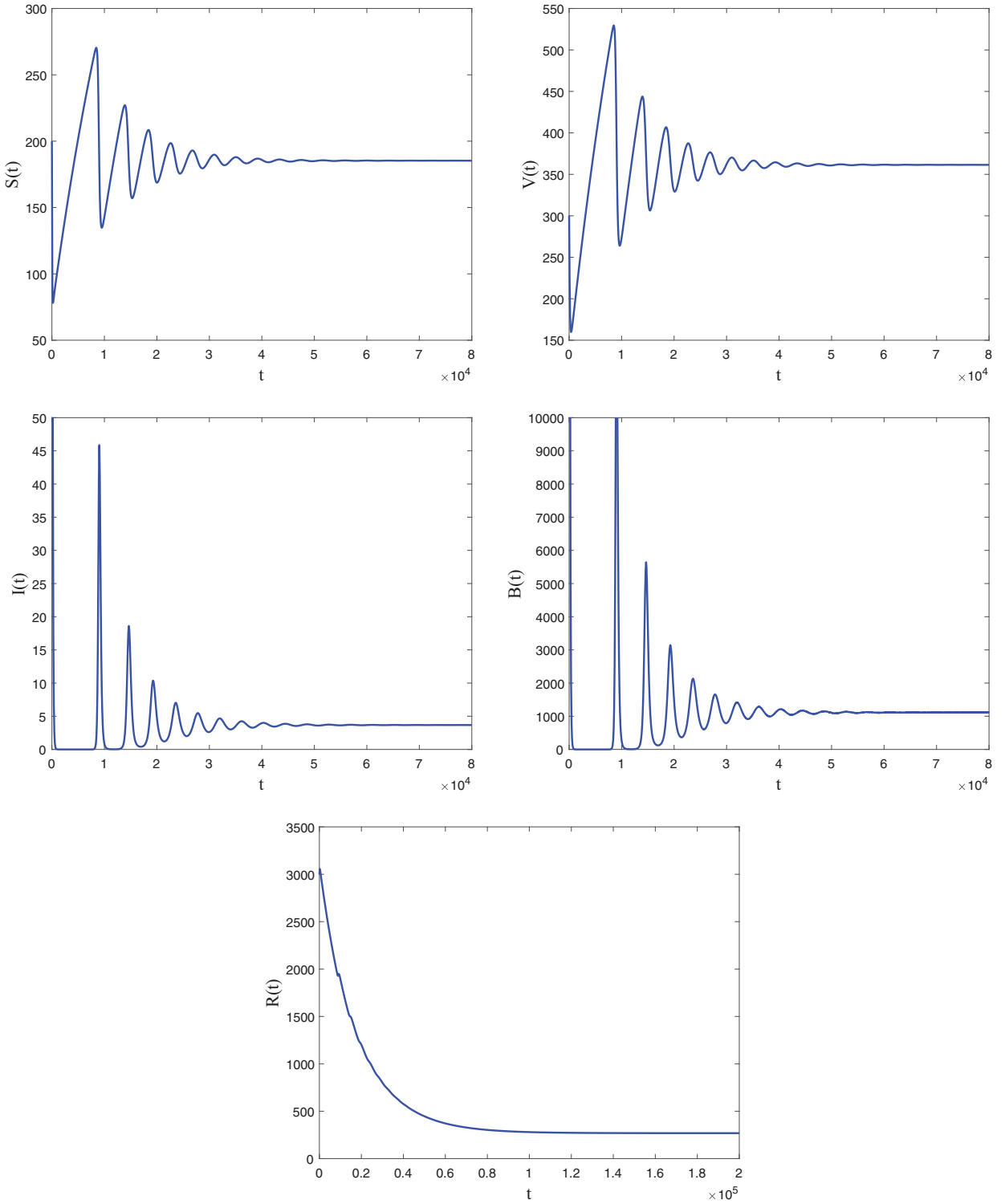

Fig. 3. The graph trajectories of $S(t)$, $V(t)$, $I(t)$, $B(t)$ and $R(t)$ versus t of system (1.2) where $\mathscr{R}_0 = 3.3274 > 1$. E^* is locally asymptotically stable.

5.2. Effect of waning rate of vaccine

Some medicine institutes have efforts on improving the vaccine efficacy. Hence, it is valuable to study the effect of the waning rate of vaccine on the dynamics of cholera infection. From Fig. 5, it is easy to see that as the waning rate

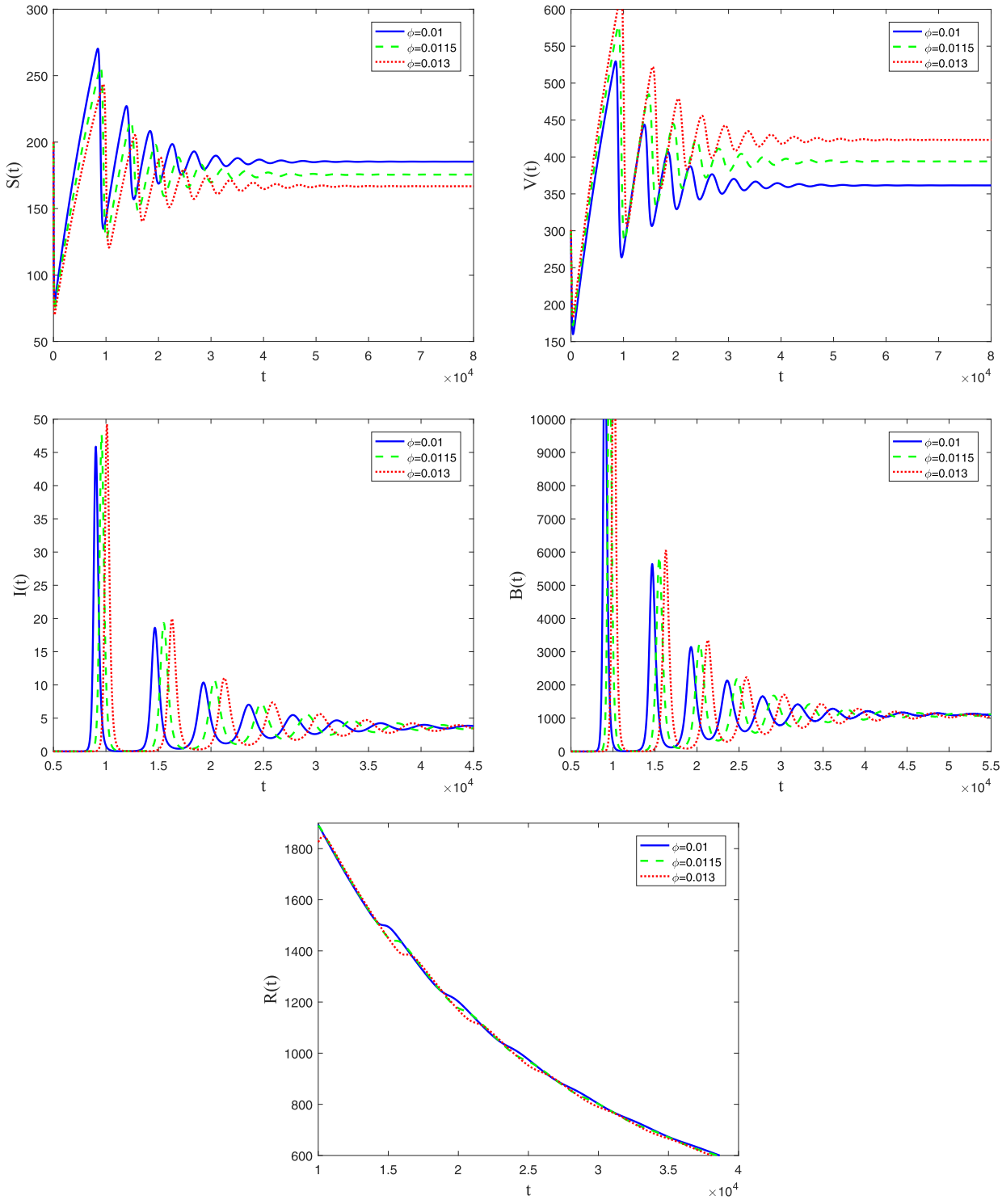

Fig. 4. The effect of ϕ on the dynamics of the model which has similar parameters and initial conditions to Fig. 3.

of vaccine η increases, susceptible individuals increases while vaccinated individuals decreases. The graph trajectories of infected individuals and pathogen population converge more quickly as η increases, which implies that the increase of the waning rate of vaccine can accelerate the infection time. Thus, to decrease the waning rate of vaccine, namely, to improve the vaccine efficacy, can delay the infection progress of cholera.

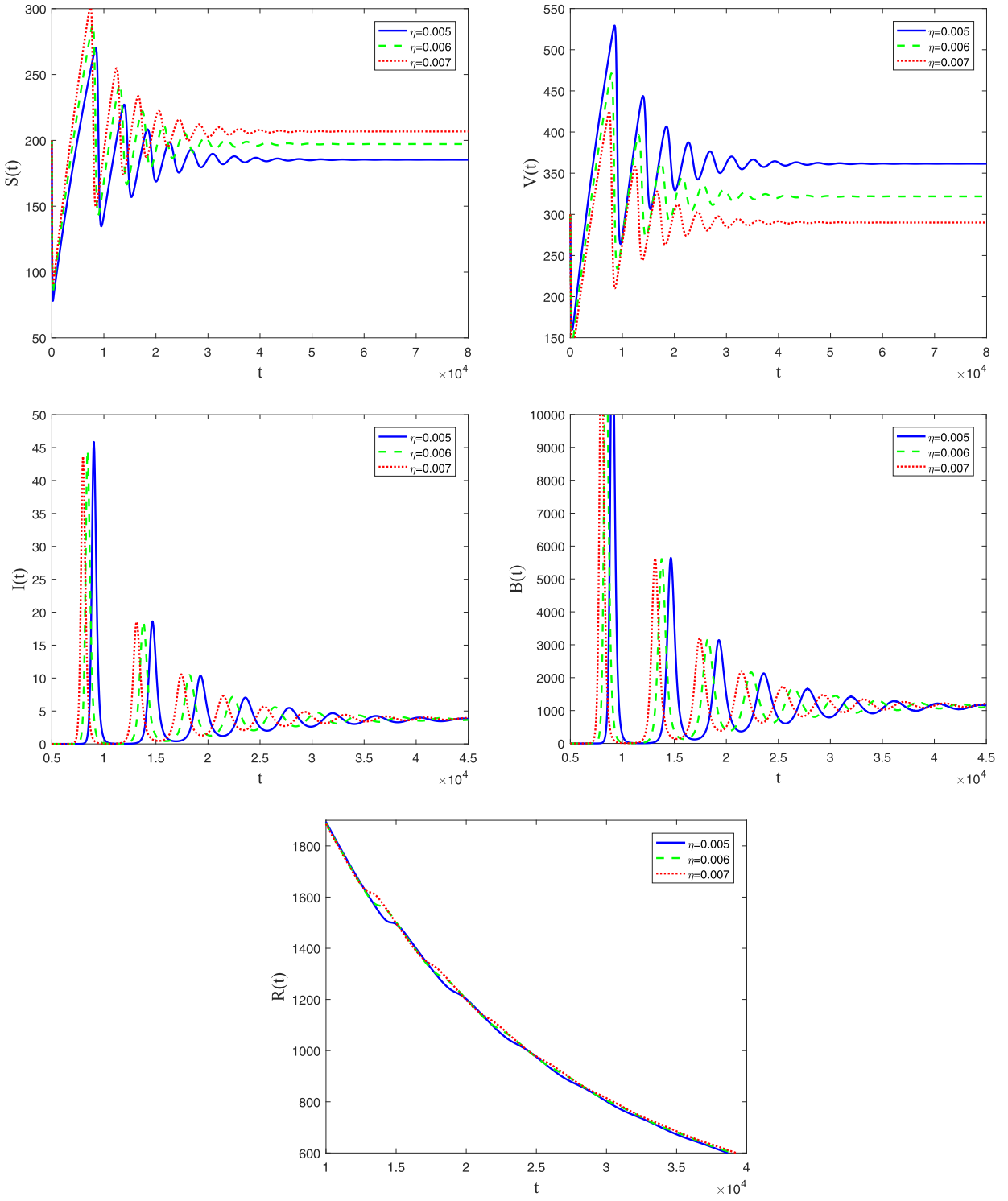

Fig. 5. The effect of η on the dynamics of the model which has similar parameters and initial conditions to Fig. 3.

5.3. Sensitivity analysis

Sensitivity analysis is used to quantify the range of variability in model responses and identify the key factors giving rise to model outcomes, which is essential for determining model robustness and reliability. Recently, Latin hypercube sampling is found to be a more efficient statistical sampling technique which has been introduced to the field of disease modelling.

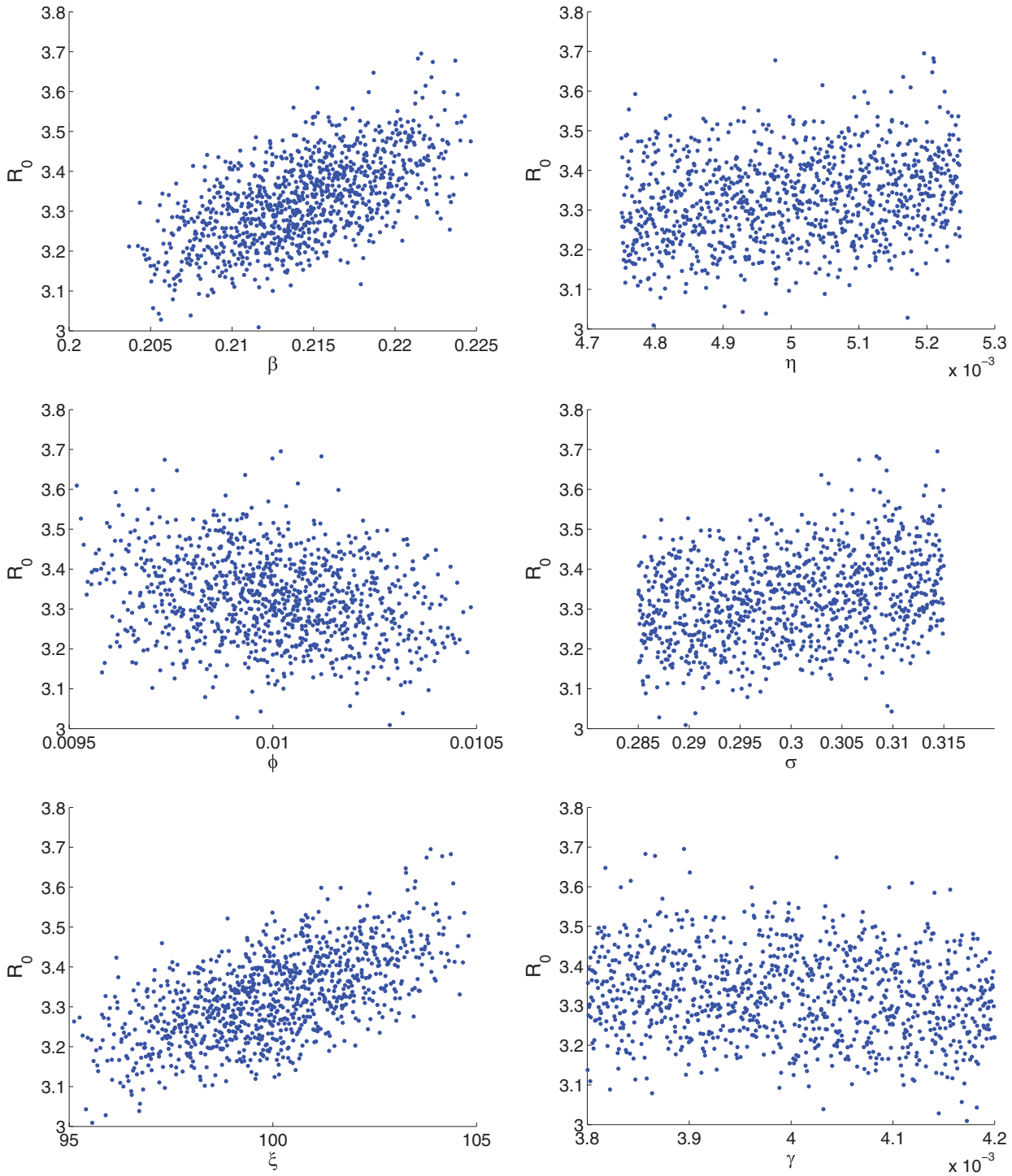

Fig. 6. Scatter plots of $\mathscr{R}_0$ with respect to β, η, ϕ, σ, ξ and γ.

Through analysis of the sample derived from Latin hypercube sampling, we can obtain large efficient data in respect to different parameters of $\mathscr{R}_0$. Fig. 6 shows the scatter plots of $\mathscr{R}_0$ in respect to β, η, ϕ, σ, ξ and γ, respectively, which implies that γ has little influence on $\mathscr{R}_0$; β, ξ, σ and η are both positive correlative variables with $\mathscr{R}_0$; ϕ is negative correlative variable with $\mathscr{R}_0$. It is worth mentioning that β contributes more to $\mathscr{R}_0$ compared to η, namely, β is a more important factor in $\mathscr{R}_0$. Fig. 7 shows a tornado plot of partial rank correlation coefficients with respect to $\mathscr{R}_0$, indicating the

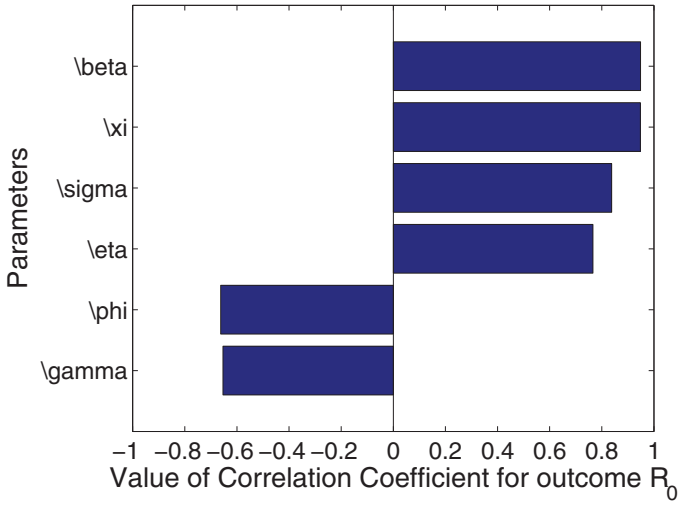

Fig. 7. Tornado plot of partial rank correlation coefficients in respect to $\mathscr{R}_0$.

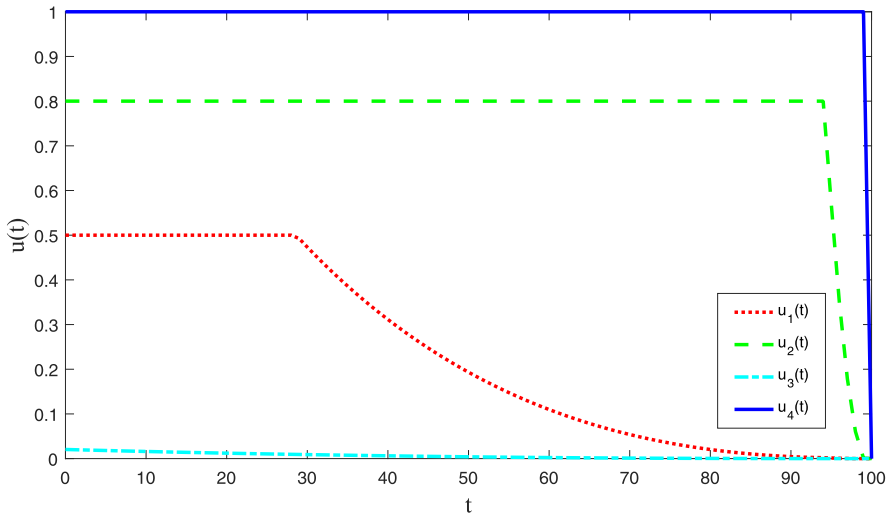

Fig. 8. The graph trajectories of four optimal control strategies.

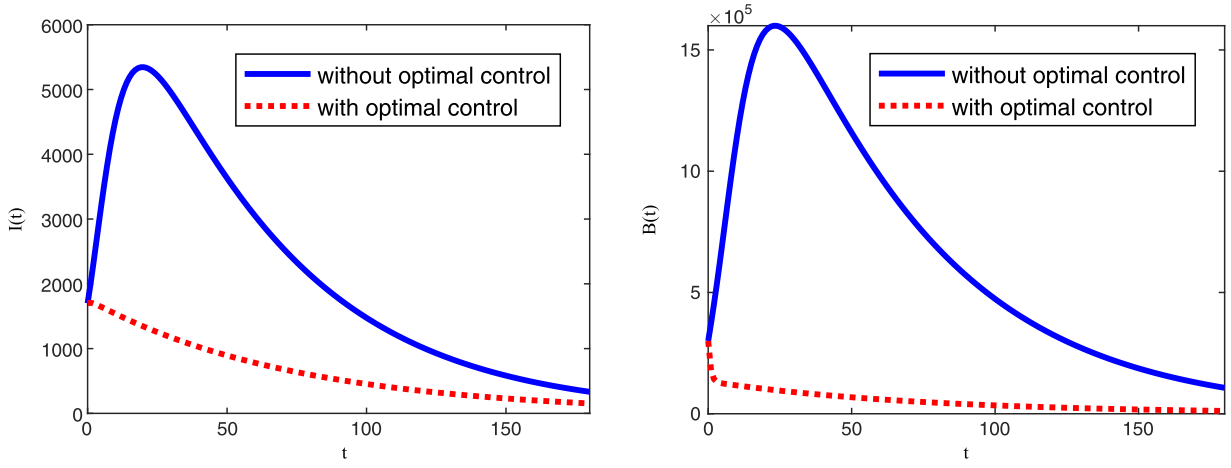

Fig. 9. The graph trajectories of $I(t)$ and $B(t)$ with optimal control and without optimal control. The initial condition is $(S(0), V(0), I(0), B(0), R(0)) = (6000, 300, 1700, 300, 000, 3000)$.

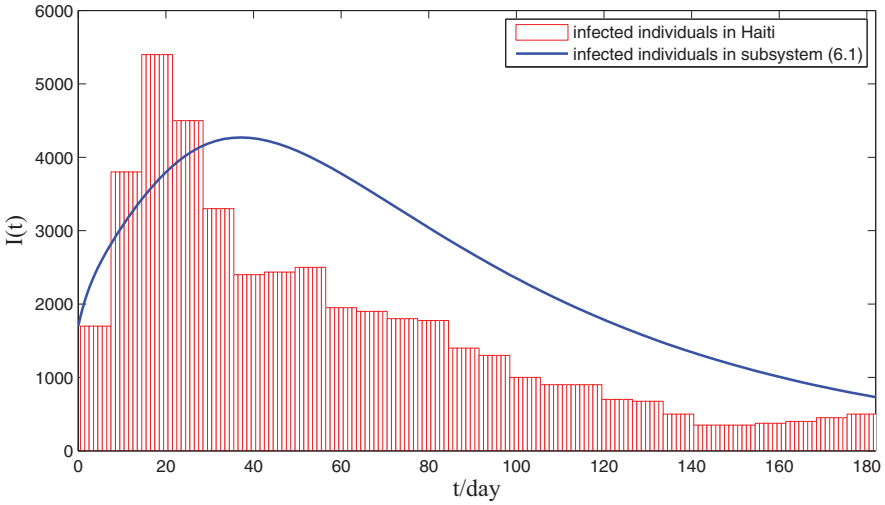

Fig. 10. The temporal solution of infectious individuals found by numerical integration of subsystem (6.1) with the same parameter values to Case 2 in Table 2 and the initial condition $(S(0), I(0), B(0)) = (6000, 1700, 300, 000)$ in which the real data [33] from the cholera outbreak in the Department of Artibonite, Haiti, from 1st November 2010 to 1st May 2011 are marked by red histogram (For interpretation of the references to color in this figure, the reader is referred to the web version of this article.).

importance of each parameter's uncertainty in contributing to $\mathscr{R}_0$ in the time to eradicate infection, which has the similar results to Fig. 6.

5.4. Optimal control solution

The numerical results associated with optimal control are obtained based on forward-backward sweep method combined with progressive-regressive Runge-Kutta fourth-order schemes [32]. A rough outline of the algorithm is given below. Here, $\vec{x} = (x_1, \ldots, x_{N+1})$ and $\vec{\lambda} = (\lambda_1, \ldots, \lambda_{N+1})$ are the vector approximations for the state and adjoint.

(1) Make an initial guess for $\vec{u}$ over the interval;

(2) Using the initial condition $x(0) = a$ and the values for $\vec{u}$, solve $\vec{x}$ forward in time according to system (4.1);

(3) Using the transversality condition $\lambda_{N+1} = \lambda(T) = 0$ and the values for $\vec{u}$ and $\vec{x}$, solve $\vec{\lambda}$ backward in time according to system (4.3);

(4) Update $\vec{u}$ by entering the new $\vec{x}$ and $\vec{\lambda}$ values into the characterization of the optimal control;

(5) Check convergence. If values of the variables in this iteration and the last iteration are negligibly close, output the current values as solutions. If values are not close, return to Step 2.

When all steps are complete, we obtain the optimal control strategies, which can be seen in Fig. 8. On account of medical technology and cost, each of control strategies has limitation, thus we set $u_{1\max} = 0.5$, $u_{2\max} = 0.8$, $u_{3\max} = 0.6$ and $u_{4\max} = 1$. We observe that $u_1(t)$, namely, vaccination strategy, could be reduced 30 days later from the beginning of the cholera outbreaks, which saves much cost of vaccination. Similarly, After 90 days, $u_2(t)$, namely, quarantine strategy, is not much necessary and could be cancelled gradually. Due to the high cost of increasing the validity of inoculation $u_3(t)$, this control strategy is not recommended. As for the sanitation strategy $u_4(t)$, it should keep in the highest level in the whole cholera epidemic.

Furthermore, in Fig. 9, we compare the number of infectious individuals as well as pathogen population with optimal control and without optimal control. It is clear that the number of infected individuals as well as pathogen population converge fast to zero due to the control strategies. At the beginning of cholera outbreak, the number of infectious individuals under the optimal control decreases from 1700–450. At the final time $T = 182$ days, the number of infectious individuals under the optimal control is the half of the number of infectious individuals without optimal control.

6. Discussion

In this paper, we have investigated the global dynamics and optimal control of a cholera infection model with environment-to-human transmission and waning vaccine-induced immunity. By analyzing corresponding characteristic equations, the local stability of each of feasible equilibria has been established. Further, the global stability of the disease-free equilibrium and the endemic equilibrium of system (1.2) has been completely established by using Lyapunov functions and LaSalle's invariance principle. By Theorem 3.1 we see that if $\mathscr{R}_0 > 1$, the endemic equilibrium is globally asymptotically stable. In this case, the disease becomes endemic. By Theorem 3.2 we see that if $\mathscr{R}_0 < 1$, the disease-free equilibrium is globally asymptotically stable. In this case, the disease will fade out.

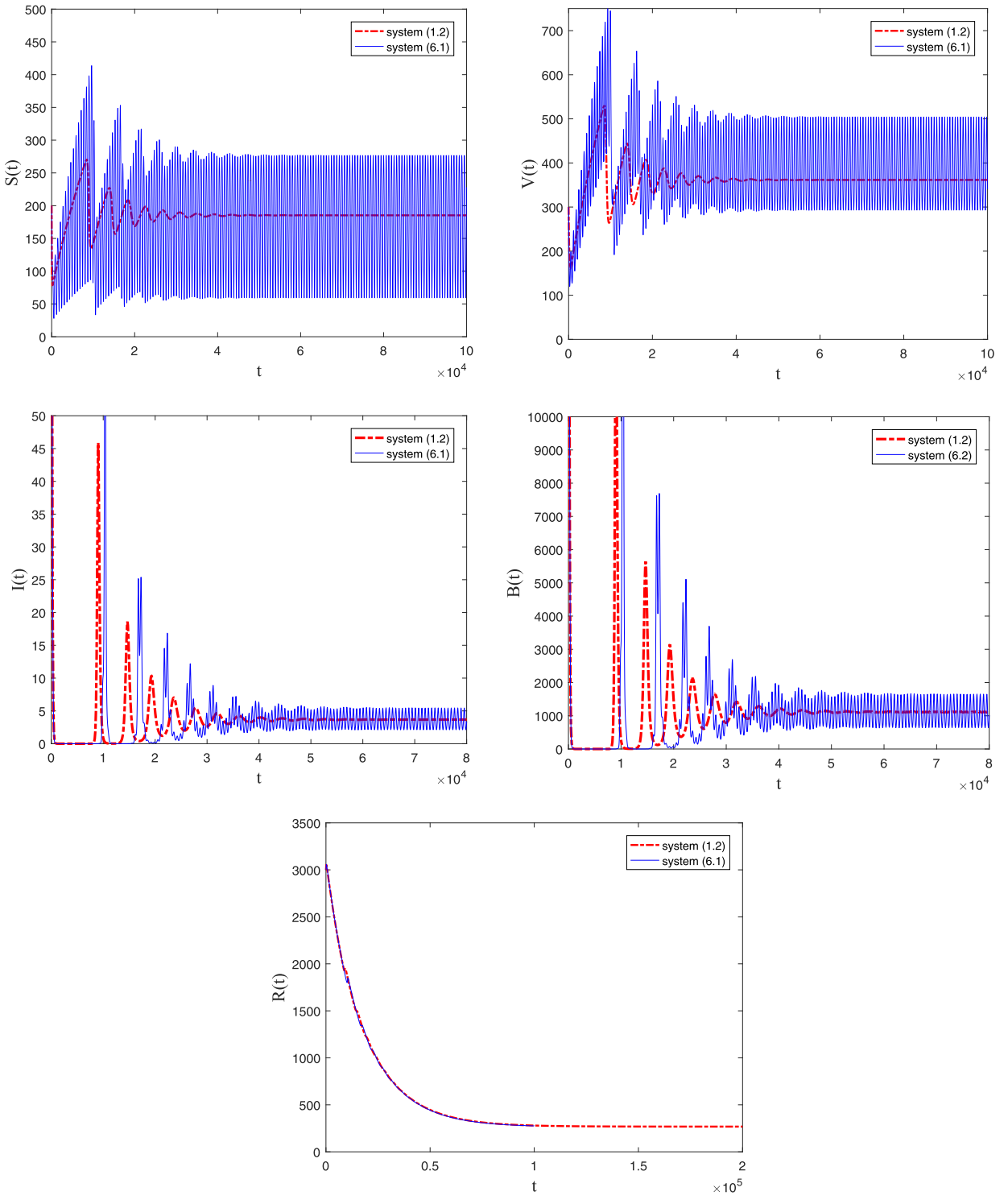

Fig. 11. The graph trajectories of $S(t)$, $V(t)$, $I(t)$, $B(t)$ and $R(t)$ versus t of system (6.2).

A recent cholera outbreak in Haiti started on 14 October 2010 in the department of Artibonite from where the disease rapidly spread along the Artibonite river affecting several departments. Within one month, all departments reported cases with a high fatality rate due to the lack of immunity and the very limited access of safe water and basic sanitation. According to the actual situation of cholera in Haiti [33], we simplify system (1.2) and let $\phi = \gamma = 0$ and $V(0) = R(0) = 0$ as follows

Table 2
Parameter values for the cholera model (1.2).

Parameter	Symbol	Case 1	Case 2	Source
Birth rate of newborns	A	$0.1/day$	$0.1/day$	Assumed
Vaccination rate	ϕ	$0.01/day$	$0.01/day$	Assumed
Environment-to-human transmission rate	β	$0.2143/day$	$0.2143/day$	[30]
Concentration of Vibrio Cholerae in environment	K	$10^6\ cells/ml$	$10^6\ cells/ml$	[30]
Waning rate of vaccine	η	$0.005/day$	$0.005/day$	Assumed
Natural human death rate	μ	$5.48\times10^{-5}/day$	$5.48\times10^{-5}/day$	[18]
The reduction of vaccine efficacy	σ	10%	30%	Assumed
Recovery rate	γ	$0.004/day$	$0.004/day$	[30,31]
Cholera-related death rate	d	$0.015/day$	$0.015/day$	[30]
Rate of human contribution to Vibrio Cholerae	ξ	20 cells/ml-per day	100 cells/ml-per day	[18]
Death rate of the vibrios	δ	$0.33/day$	$0.33/day$	Assumed

$$\begin{aligned}
\dot{S}(t) &= A - \frac{\beta S(t)B(t)}{K+B(t)} - \mu S(t),\\
\dot{I}(t) &= \frac{\beta S(t)B(t)}{K+B(t)} - (\mu+d)I(t),\\
\dot{B}(t) &= \xi I(t) - \delta B(t),
\end{aligned} \tag{6.1}$$

In Fig. 10, the red histogram denotes the cholera cases occurred in Artibonite, while the blue curve represents the numerical simulation curve of subsystem (6.1). Fig. 10 indicates that the simulation of model agrees well with the real data reported.

We would like to mention here that in this paper, we only considered the case that waning rate is constant. In general, vaccines can wear off, however, it's not right after individuals are vaccinated. In the following, we use a periodic type for the waning rate instead and system (1.2) can be rewritten as

$$\begin{aligned}
\dot{S}(t) &= A - \phi S(t) - \frac{\beta S(t)B(t)}{K+B(t)} - \mu S(t) + \eta(t)V(t),\\
\dot{V}(t) &= \phi S(t) - \frac{\sigma\beta V(t)B(t)}{K+B(t)} - (\mu+\eta(t))V(t),\\
\dot{I}(t) &= \frac{\beta S(t)B(t)}{K+B(t)} + \frac{\sigma\beta V(t)B(t)}{K+B(t)} - (\mu+\gamma+d)I(t),\\
\dot{B}(t) &= \xi I(t) - \delta B(t),\\
\dot{R}(t) &= \gamma I(t) - \mu R(t).
\end{aligned} \tag{6.2}$$

In order to evaluate the effect of $\eta(t)$ on the infection dynamics, we let $\eta(t) = 0.005(1+\sin(0.01t))$ and other parameters remain unchanged. From Fig. 11, we observe that system (6.2) admits rich and complex dynamics including periodic solutions. It is interesting to carry out a complete mathematical analysis of system (6.2) when we choose the periodic type waning rate. We leave this for our future work.

Acknowledgments

This work was supported by the National Natural Science Foundation of China (Nos.11871316,11801340,11501340), the Natural Science Foundation of Shanxi Province of China (201801D121006,201801D221007), Shanxi Scientific Data Sharing Platform for Animal Diseases (201605D121014), and the Science and Technology Innovation Team of Shanxi Province (201605D131044-06).

References

[1] Z. Mukandavire, A. Tripathi, C. Chiyaka, et al., Modelling and analysis of the intrinsic dynamics of cholera, Differ. Equ. Dyn. Syst. 19 (2011) 253–256.
[2] E.J. Nelson, J.B. Harris, J.G. Morris, et al., Cholera transmission: the host, pathogen and bacteriophage dynamics, Natl. Rev. Microbiol. 7 (2009) 693–702.
[3] World health organzation, http://www.emro.who.int/pandemic-epidemic-diseases/cholera/weekly-update-cholera-in-yemen-06-july-2017.html.
[4] V. Capasso, S.L. Paveri-Fontana, A mathematical model for the 1973 cholera epidemic in the european mediterranean region, Rev. Epidemiol. Sante Publique 27 (1973) 121–132.
[5] R.R. Colwell, A. Huq, Environmental reservoir of vibrio cholera, the causative agent of cholera, Ann. New York Acad. Sci. 740 (1994) 44–54.
[6] C.T. Codeço, Endemic and epidemic dynamics of cholera: the role of the aquatic reservoir, BMC Infect. Dis. 1 (2001) 1–14.
[7] T.K. Sengupta, R.K. Nandy, S. Mukhopadyay, et al., Characterization of a 20-kda pilus protein expressed by a diarrheogenic strain of non-o1/non-o139 vibrio cholerae, FEMS Microbiol. Lett. 160 (1998) 183–189.
[8] Y. Cheng, J. Wang, X. Yang, On the global stability of a generalized cholera epidemiological model, J. Biol. Dyn. 6 (2012) 1088–1104.
[9] S.D. Hove-Musekwa, F. Nyabadzac, C. Chiyaka, et al., Modelling and analysis of the effects of malnutrition in the spread of cholera, Math. Comput. Model. 53 (2011) 1583–1595.
[10] S. Liao, J. Wang, Stability analysis and application of a mathematical cholera model, Math. Biosci. Eng. 8 (2011) 733–752.
[11] Z. Mukandavire, S. Liao, J. Wang, et al., Estimating the reproductive numbers for the 2008–2009 cholera outbreaks in zimbabwe, Proc. Natl. Acad. Sci. 108 (2011) 8767–8772.

[12] P. Panja, S.K. Mondal, J. Chattopadhyay, Dynamics of cholera outbreak with bacteriophage and periodic rate of contact, Int. J. Dyn. Control 4 (2016) 284–292.
[13] J.P. Tian, J. Wang, Global stability for cholera epidemic models, Math. Biosci. 232 (2011) 31–41.
[14] Y. Wang, J. Wei, Global dynamics of a cholera model with time delay, Int. J. Biomath. 6 (2013) 18. 1250070
[15] M. Jeuland, J. Cook, C. Poulos, et al., Cost-effectiveness of new-generation oral cholera vaccines: a multisite analysis, Value Health 12 (2009) 899–908.
[16] S. Liao, W. Yang, Optimal control and stability analysis of cholera model with vaccination, J. Syst. Sci. Math. Sci. 36 (2016) 2257–2271.
[17] C. Modnak, J. Wang, Z. Mukandavire, Simulating optimal vaccination times during cholera outbreaks, Int. J. Biomath. 7 (2014) 12. 1450014
[18] C. Modnak, A model of cholera transmission with hyperinfectivity and its optimal vaccination control, Int. J. Biomath. 10 (2017) 16. 1750084
[19] D. Posny, J. Wang, Z. Mukandavire, C. Modnak, Analyzing transmission dynamics of cholera with public health interventions, Math. Biosci. 264 (2015) 38–53.
[20] X. Zhou, J. Cui, Z. Zhang, Global results for a cholera model with imperfect vaccination, J. Frankl. Inst. 349 (2012) 770–791.
[21] P. van den Driessche, J. Watmough, Reproduction numbers and sub-threshold endemic equilibria for compartmental models of disease transmission, Math. Biosci. 180 (2002) 29–48.
[22] J.K.K. Asamoah, F.T. Oduro, E. Bonyah, et al., Modelling of rabies transmission dynamics using optimal control analysis, J. Appl. Math. 12 (2017) 1–23.
[23] L. Pontryagin, V. Boltyanskii, R. Gramkrelidze, E. Mischenko, The Mathematical Theory of Optimal Processes, Wiley Interscience, 1962.
[24] L. Cesari, Optimization-Theory and Applications: Problems with Ordinary Differential Equations, SpringerVerlag, New York, 1983.
[25] W.H. Fleming, R.W. Rishel, Deterministic and Stochastic Optimal Control, Springer Verlag, New York, 1975.
[26] A.P. Lemos-Paião, C.J. Silva, D.F.M. Torres, An epidemic model for cholera with optimal control treatment, J. Comput. Appl. Math. 318 (2017) 168–180.
[27] C.J. Silva, D.F.M. Torres, Optimal control for a tuberculosis model with reinfection and post-exposure interventions, Math. Biosci. 244 (2013) 154–164.
[28] M. McAsey, L. Mou, W. Han, Convergence of the forward-backward sweep method in optimal control, Comput. Optim. Appl. 53 (2012) 207–226.
[29] O. Zakary, A. Larrache, M. Rachik, et al., Effect of awareness programs and travel-blocking operations in the control of HIV/AIDS outbreaks: a multi–domains SIR model, Adv. Differ. Equ. 2016 (2016) 169.
[30] D.M. Hartley, J.G. Morris Jr., D.L. Smith, Hyperinfectivity: a critical element in the ability of v. cholerae to cause epidemics? PLoS Med. 3 (2006) 0063–0069.
[31] T.R. Hendrix, The pathophysiology of cholera, Bull. NewYork Acad. Med. 47 (1971) 1169–1180.
[32] S. Lenhart, J.T. Workman, Optimal control applied to biological models, Chapman & Hall/CRC Press, Boca Raton, 2007.
[33] World Health Organization, Global Task Force on Cholera Control, Cholera Country Profile: Haiti, 18 may, World health Organization, 2011, http://www.who.int/cholera/countries/HaitiCountryProfileMay2011.pdf.